# A generating mechanism for higher order rogue waves

J.S.He [1], H.R. Zhang [1], L.H. Wang [1], K. Porsezian [2] and A.S.Fokas[3,4]
[1] *Department of Mathematics, Ningbo University, Ningbo, Zhejiang 315211 P.R. China.*
[2] *Department of Physics, Pondicherry University, Puducherry 605014 India*
[3] *School of Engineering and Applied Sciences, Harvard University, Cambridge, MA 02138,USA.*
[4] *Permanent address:DAMTP, University of Cambridge, Cambridge, CB3 0WA, UK*

We introduce a mechanism for generating higher order rogue waves (HRWs) of the nonlinear Schrödinger(NLS) equation: the progressive fusion and fission of $n$ degenerate breathers associated with a critical eigenvalue $\lambda_0$ creates an order-$n$ HRW. By adjusting the relative phase of the breathers in the interacting area, it is possible to obtain different types of HRWs. The value $\lambda_0$ is a zero point of an eigenfunction of the Lax pair of the NLS equation and it corresponds to the limit of the period of the breather tending to infinity. By employing this mechanism we prove two conjectures regarding the total number of peaks, as well as a decomposition rule in the circular pattern of an order-$n$ HRW.
KEYWORDS: rogue wave, breather, nonlinear Schrödinger equation.

PACS numbers: 42.65.Tg,42.65.Sf,05.45.Yv,02.30.Ik



**Introduction.** Rogue waves(RWs) in the ocean are catastrophic natural phenomena with a long history and fascinating mariner stories [1]. Detailed studies of RWs have occurred only during the past five decades [2–5]. A prototype one dimensional rogue wave is the so-called Peregrine soliton [6]; this soliton exhibits the two remarkable characteristics of first-order RWs: (a) localized behavior in both space and time, (b) the existence of one dominant peak. RWs have been observed in several fields, including optics [7–9], superfluid helium [10], Bose-Einstein condensates [11], plasmas [12, 13], microwaves [14], capillary phenomena[15], telecommunication data streams [16], and inhomogeneous media [17].

A typical modeling equation for RWs in fiber optics is the celebrated nonlinear Schrödinger (NLS) equation [18],

$$iq_t + q_{xx} + 2|q|^2 q = 0. \tag{1}$$

Here $q = q(x,t)$ is a complex smooth function of $x$ and $t$, and the subscripts denote partial derivatives. The Peregrine soliton [6], which is the first-order RW [19] of the NLS equation, has been observed experimentally in fibers [20], in a water tank [21], and in multi-component plasmas [22]. Recently, a super rogue wave [23], i.e., a second order RW, has also been observed in a water tank. In addition to the NLS equation, the Hirota equation [24, 25], the first-type derivative NLS(DNLS) equation [26], the third type DNLS equation [27], the NLS-Maxwell-Bloch equations [28], the discrete NLS equation [29], the two-component NLS equations [30–32], and the Davey-Stewartson equation [33, 34], also admit RWs. These results show that RWs may be generic phenomena in nonlinear systems.

The Peregrine soliton [6, 19] of the NLS equation is expressed in terms of a simple rational formula; it corresponds to a simple profile and can be obtained from a breather solution via the simple limit of the period of modulation approaching infinity. However, higher order rogue waves(HRWs) [35–38] are expressed in terms of complicated formulas and their profiles exhibit several different interesting patterns [39–43]. These patterns include a fundamental pattern consisting of a simple central highest peak surrounded by several gradually decreasing peaks [see Figs. 2(a) and 3 in Ref.[43]], an equal-height triangular pattern [see Fig. 2(b) in Ref. [43] and Fig.2 in Ref. [40]], and circular pattern [see Fig.4 in Ref. [43]].

Taking into consideration the complexity of the relevant formulas [44, 45], as well as the plethora of different possible patterns, it is a challenging problem to elucidate the mechanism of HRW generation. There exist two important conjectures regarding HRWs.

- In the case of a single fundamental pattern, an order-$n$ RW has $n(n+1)-1$ non-uniform peaks [43]; in the case when there exist several patterns, an order-$n$ RW has $n(n+1)/2$ uniform peaks [36, 37].
- In the case when an order-$n$ RW displays a ring structure, the outer ring has $2n-1$ uniform peaks, and the inner structure is an order-$(n-2)$ RW[43].

In this work, we present a generating mechanism for HRWs of the NLS equation, and using this mechanism, we prove the above two conjectures. Furthermore, we discuss several new interesting patterns of HRWs.

**A Degenerate n-fold DT and inverse DT.** In order to study the breather and the RW solutions of the NLS equation, we shall use the determinant representation of the Darboux transformation (DT) introduced in [46–48]. Furthermore, we shall use the notations and the main results of these references regarding the $n$-fold DT (theorem 1 in [48]) and the related functions $(q^{[n]}, r^{[n]}, \phi^{[n]})$ generated by the n-fold DT(corollary 1 in [48]). In order to satisfy the reduction requirement $q^{[n]} = -(r^{[n]})^*$,we choose $f_{2k} = (-f^*_{2k-1\ 2}, f^*_{2k-1\ 1})^T, k = 1, 2, \cdots, n$, where $T$ denotes matrix transposition and the asterisk denotes complex conjugation. Under this reduction, $q^{[n]}$ is a solution of the NLS equation generated by an $n$-fold DT starting with the seed solution $q$. In the following we always use this reduction condition.

Theorem 1 and corollary 1 cited above imply that an $n$-fold DT $T_n$ of the NLS equation annihilates its independent generating functions, which are the eigenfunctions $f_i (i = 1, 3, 5 \cdots, 2n-1)$ associated with $n$ distinct eigenvalues $\lambda_1, \lambda_3, \lambda_5, \cdots, \lambda_{2n-1}$. This means that if we fix the given set of eigenvalues, we cannot apply DTs more than once. Recall that the formulas for the eigenfunctions $f_i (i = 1, 3, 5 \cdots, 2n-1)$ differ only by the fact that they involve different eigenvalues $\lambda_i$. However, in order to obtain a HRW for a critical eigenvalue $\lambda_0$, we must apply repeated DTs. This difficulty can be overcome by noting that the annihilated eigenfunctions can be re-created

by taking the limit $\lambda_i \to \lambda_1$ of the eigenvalues used in the DT [40]. We set $f_i = \phi(\lambda_i)$ and $f_i^{[n]} = \phi^{[n]}|_{\lambda=\lambda_i}$. We shall use the determinant representation of the $n$-fold DT [see Eq. (14) of [48]] to illustrate the relevant construction. It is straightforward to verify that $f_1^{[1]} = 0$, and hence we cannot apply the DT again with the eigenvalue $\lambda_1$. Let $\lambda_3 = \lambda_1 + \epsilon$; then

$$\begin{aligned} f_3^{[1]} &= f_3^{[1]}(\lambda_1+\epsilon) = f_1^{[1]}(\lambda_1+\epsilon) \\ &= f_1^{[1]}(\lambda_1) + \left(\frac{\partial f_1^{[1]}(\lambda_1+\epsilon)}{\partial\epsilon}|_{\epsilon=0}\right)\epsilon + O(\epsilon). \end{aligned}$$

Hence, the limit

$$\lim_{\epsilon\to 0}\frac{1}{\epsilon}f_3^{[1]} = \frac{\partial f_1^{[1]}(\lambda_1+\epsilon)}{\partial\epsilon}|_{\epsilon=0} \triangleq f_1^{[1]}$$

yields a transformed eigenfunction associated with $\lambda_1$, which can be used to generate a new DT so that we can apply this DT with the given eigenvalue $\lambda_1$ for a second time. Similarly, set the second degenerate eigenvalue $\lambda_5 = \lambda_1 + \epsilon$ in $f_5^{[2]}$; the limit

$$\lim_{\epsilon\to 0}\frac{1}{\epsilon^2}f_5^{[2]} = \frac{\partial^2 f_1^{[2]}(\lambda_1+\epsilon)}{\partial\epsilon^2}|_{\epsilon=0} \triangleq f_1^{[2]}$$

re-creates a transformed eigenfunction associated with $\lambda_1$ of the two-fold DT. Note that the zero order and the first order terms of $\epsilon$ in $f_5^{[2]}$ yield zero contributions. In general, for an $n$-fold DT, we can use the following theorem on $\phi^{[n]}(\lambda)$ and $q^{[n]}$ using the degenerate limit $\lambda_i \to \lambda_1$ by a similar analysis, based on the determinant representation given by Theorem 1 and Corollary 1 of [48]. The following notations, including matrix elements $[(t_1)_{12}]_{ij}$ and $(W_{2n})_{ij}$, are given in [48].

**Theorem 1** *An n-fold DT with a given eigenvalue $\lambda_1$ is realized by the degenerate limit $\lambda_i \to \lambda_1$. This degenerate n-fold DT yields the transformed eigenfunction $\phi^{[n]}$ of $\lambda$,where*

$$\phi^{[n]} = \frac{1}{|W'_{2n}|}\begin{pmatrix} \begin{vmatrix} \hat{\phi}(n) & \lambda^n\phi_1 \\ W'_{2n} & \hat{\xi}'_{2n-1} \end{vmatrix} \\ \begin{vmatrix} \hat{\phi}(n) & \lambda^n\phi_2 \\ W'_{2n} & \hat{\xi}'_{2n} \end{vmatrix} \end{pmatrix}, \tag{2}$$

*as well as a new solution $q^{[n]}$ of the NLS equation starting with the seed solution $q$,where*

$$q^{[n]}(x,t;\lambda_1) = q - 2i\frac{|Q'_{2n}|}{|W'_{2n}|}, \tag{3}$$

*with*

$$\begin{aligned} W'_{2n} &= \left(\frac{\partial^{n_i-1}}{\partial\varepsilon^{n_i-1}}\Big|_{\varepsilon=0}(W_{2n})_{ij}(\lambda_1+\epsilon)\right)_{2n\times 2n}, \\ \hat{\xi}'_{2n-1} &= \left(\frac{\partial^{n_i-1}}{\partial\varepsilon^{n_i-1}}\Big|_{\varepsilon=0}\hat{\xi}_{2n-1,i}(\lambda_1+\epsilon)\right)_{2n\times 1}, \\ \hat{\xi}'_{2n} &= \left(\frac{\partial^{n_i-1}}{\partial\varepsilon^{n_i-1}}\Big|_{\varepsilon=0}\hat{\xi}_{2n,i}(\lambda_1+\epsilon)\right)_{2n\times 1}, \\ Q'_{2n} &= \left(\frac{\partial^{n_i-1}}{\partial\varepsilon^{n_i-1}}\Big|_{\varepsilon=0}(Q_{2n})_{ij}(\lambda_1+\epsilon)\right)_{2n\times 2n}, \end{aligned}$$

*$n_i = [\frac{i+1}{2}]$, $[i]$ denotes the floor function of $i$, $Q_{2n}$ is the determinant in the numerator of $(t_1)_{12}$[48].*

Starting with different seed solutions $q$, Eq. (3) yields different degenerate solitons and breathers. Furthermore, by choosing a special eigenvalue $\lambda_1 = \lambda_0$ associated with $\phi(\lambda_0) = 0$ , Eq. (3) yields an order $n$ RW. In the latter case, all orders of derivatives with respect to $\epsilon$ in $\phi^{[n]}$ and $q^{[n]}(x,t;\lambda_1)$ are increased by 1 because $\phi(\lambda_0) = 0$. The main idea of the above procedure for constructing rogue wave is the following: According to the determinant representation in Theorem 1 and Corollary 1 of [48], there are two degenerate cases in $T_{2k}$, i.e., $\lambda_i \to \lambda_1$ and $f_i = \phi(\lambda_i) = 0 (i = 1, 3, \cdots, 2k-1)$. It is easy to recognize that $q^{[2k]}$ generated by $T_{2k}$ is given by an indeterminate form $\frac{0}{0}$ in the above degenerate cases. Thus, whether $\lambda_i = \lambda_1 + \epsilon$ or $\lambda_i = \lambda_0 + \epsilon$ , smooth solutions can be obtained by higher-order Taylor expansion in determinants with respect to $\epsilon$ as in Theorem 1.

In order to get an order-$(n-2)$ RW from an order-$n$ RW by a simple limit, it is necessary to use an inverse DT. For a general eigenvalue $\lambda$, the $x$ part of the Lax pair of the NLS equation admits the solution $\phi(\lambda)$, as well as the linearly independent solution $\psi(\lambda) = (\psi_1, \psi_2)^T$. Furthermore $\psi^{[n]} = T_n\psi$ and $\phi^{[n]} = T_n\phi$ are linearly independent because $T_n$ is a linear transformation of $\psi$ and $\phi$. Let $g_k \triangleq (g_{k1}, g_{k2})^T = \psi(\lambda_k)$; then the Wronskian determinant $W(f_i, g_i) = f_{i1}g_{i2} - f_{i2}g_{i1}$ of $f_i$ and $g_i$ is a non-zero constant. Using the determinant representation of the one-fold DT, $T(\lambda; f_1, f_2)$, generated by $f_1$ and $f_2$, we find the transformed functions

$$\begin{aligned} g_1^{[1]} &= \frac{(\lambda_1-\lambda_2)W(f_1,g_1)}{|W_2|}\begin{pmatrix} f_{21} \\ f_{22} \end{pmatrix}, \\ g_2^{[1]} &= \frac{(\lambda_1-\lambda_2)W(f_2,g_2)}{|W_2|}\begin{pmatrix} f_{11} \\ f_{12} \end{pmatrix}, \end{aligned}$$

which are not zero in contrast to $f_1^{[1]} = 0$ and $f_2^{[2]} = 0$. Hence, we can use $g_1^{[1]}$ and $g_2^{[1]}$ to generate the second fold DT $T(\lambda; g_1^{[1]}, g_2^{[2]})$. Using a straightforward calculation with the help of Theorem 1 in [48], it can be shown that the two-fold DT is given by

$$T_2 = T(\lambda; g_1^{[1]}, g_2^{[1]})T(\lambda; f_1, f_2) = (\lambda-\lambda_1)(\lambda-\lambda_2)I, \tag{4}$$

where $I$ is the unit matrix of size 2. Here we present only the calculation of the element $(T_2)_{11}$. First note that

$$\begin{aligned} &|W_4(g_1, g_2, f_1, f_2)| = -(\lambda_2-\lambda_1)^2 W(f_1,g_1)W(f_2,g_2); \\ &(\tilde{T}_2)_{11} = -(\lambda-\lambda_1)(\lambda-\lambda_2)(\lambda_2-\lambda_1)^2 W(f_1,g_1)W(f_2,g_2). \end{aligned}$$

Hence,

$$(T_2)_{11} = \frac{(\tilde{T}_2)_{11}}{|W_4(g_1,g_2,f_1,f_2)|} = (\lambda-\lambda_1)(\lambda-\lambda_2).$$

Thus $T(\lambda; g_1^{[1]}, g_2^{[1]})$ is the inverse DT of $T(\lambda; f_1, f_2)$. In general, for an $(n-2)$-fold DT $T_{n-2}$ generated by $f_1, f_2, \ldots, f_{2n-5}, f_{2n-4}$, we can find a one-fold inverse DT as follows(note that $g_{2n-3}^{[n-2]} = T_{n-2}g_{2n-3}$ or $g_{2n-2}^{[n-2]} = T_{n-2}g_{2n-2}$ and $f_{2n-3}^{[n-2]}$or $f_{2n-2}^{[n-2]}$ are linearly independent):

**Theorem 2** *Let the $(n-1)$-th fold DT be $T(\lambda; f_{2n-3}^{[n-2]}, f_{2n-2}^{[n-2]})$ after an (n-2)-fold DT $T_{n-2}$,*

*and* $g_{2n-3}^{[n-1]} = T(\lambda; f_{2n-3}^{[n-2]}, f_{2n-2}^{[n-2]}) g_{2n-3}^{[n-2]}, g_{2n-2}^{[n-1]} = T(\lambda; f_{2n-3}^{[n-2]}, f_{2n-2}^{[n-2]}) g_{2n-2}^{[n-2]}$. *Then the n-th fold DT* $T(\lambda; g_{2n-3}^{[n-1]}, g_{2n-2}^{[n-1]})$ *is the inverse of the* $(n-1)$*-th fold DT.*

In other words, the n-th fold DT $T(\lambda; g_{2n-3}^{[n-1]}, g_{2n-2}^{[n-1]})$ maps $q^{[n-1]}$ to $q^{[n-2]}$. This gives an important connection between RWs of order $(n-1)$ and order $(n-2)$.

**Higher order breathers and rogue waves** The first-order breather of the NLS equation is a periodic traveling wave. This solution, via the limit of the period approaching infinity, gives the first-order RW [6, 19]. However, it is still not clear how to generate HRWs from multi-breathers, even for second-order RWs [41]. Moreover, the collision of three breathers [49] does not provide a satisfactory explanation for the appearance of different patterns of order-3 RWs.

On the $(x,t)$ plane, because of the conservation of the number of breathers, there exist $n$ separate peaks in each row before and after the interaction of $n$ breathers. The interaction area is localized near the origin of the plane between the two closest rows (or periods) possessing $n$ separate peaks. When the breathers are in the interaction area, their peaks get closer. Based on the detailed investigation of the interaction of breathers, we claim the following mechanism for the generation of HRWs: the progressive fusion and fission of $n$ degenerate breathers associated with a critical eigenvalue $\lambda_0$ creates an order-$n$ HRW. Furthermore, by adjusting the relative phase of the breathers in the interacting area, it is possible to obtain different patterns of HRWs. Here $\lambda_0$ is a zero point of the eigenfunction $\phi(\lambda)$, i.e., $\phi(\lambda_0) = 0$, which corresponds to the limit of the period of the breathers becoming infinitely large. The relative phase can be adjusted via the tuning of the parameters $s_i$ in the eigenfunctions $f_i$.

In this work, we shall take a periodic seed $q = ce^{\mathbf{i}\rho}$ with $\rho = ax + (2c^2 - a^2)t$. The corresponding eigenfunctions $\phi(\lambda) = (\phi_1, \phi_2)^T$ are given by

$$\phi(\lambda)=\begin{pmatrix} ce^{\mathbf{i}(\frac{\rho}{2}+d(\lambda))}+\mathbf{i}(\frac{a}{2}+c_1(\lambda)+\lambda)e^{-\mathbf{i}(-\frac{\rho}{2}+d(\lambda))} \\ ce^{-\mathbf{i}(\frac{\rho}{2}+d(\lambda))}+\mathbf{i}(\frac{a}{2}+c_1(\lambda)+\lambda)e^{\mathbf{i}(-\frac{\rho}{2}+d(\lambda))} \end{pmatrix}. \quad (5)$$

Here $c_1(\lambda) = \sqrt{c^2 + (\lambda + a/2)^2}, d(\lambda) = c_1(\lambda)(x + (2\lambda - a)t + s_0 + \Phi), \Phi = \sum_{k=1}^{n-1} s_k \epsilon^{2k}$[40], $n$ denotes the number of steps of the multi-fold DT, $\lambda_0 = -a/2 + ic$ is a zero point of the eigenfunction $\phi(\lambda)$, $\epsilon$ denotes a small parameter when we consider the degeneracy of the eigenvalues,i.e., $\lambda = \lambda_0 + \epsilon$, and $s_i$ are complex constants. The functions $f_i = \phi(\lambda_i)$ have the same form except for the occurrence of different values of the eigenvalues which is necessary to generate HRWs via the process of eigenvalue degeneration $\lambda_i \mapsto \lambda_1$ (see Theorem 1). In the following examples we set $a = 0$. Also, in order to adjust the relative phase of the breathers in the interaction area according to Theorem 1 and Corollary 1 of Ref. [48], we set $s_i = 0 (i \geq 1)$, but $s_0$ has different values in different $f_i$. There exist three types of relative phases of $n$ breathers in the interaction area: synchronous, anti-synchronous, and quasi-synchronous.

In the interaction area of $n$ synchronous breathers, there exist progressively increasing fusion via $n-1$ steps from the $n$ lower peaks to the central maximum peak, and then progressively decreasing fission via $n-1$ steps from the central maximum peak to the $n$ lower peaks. Here, each step of fusion annihilates one peak and hence the height of the peaks increases; similarly, each step of fission creates one new peak and hence the height of the peaks decreases. These peaks are arranged as two triangles with one joint vertex along their perpendicular bisector. Thus, the total number of non-uniform peaks in the interaction area is $n(n+1)-1$. It is interesting to note that the outermost row of the interaction area has $n$ lower peaks, which are close to each other. Hence, the peaks are much lower than the ones in the nearest row of the non-interaction area. This phenomenon provides evidence for the strong interaction of the breathers. When the eigenvalue used in the breathers approaches the critical value $\lambda_0$,i.e. $\lambda_i \mapsto \lambda_0$, the periods of all breathers go to infinity simultaneously, so that only one profile in the interaction area survives, and this gives the fundamental pattern of a HRW. Therefore, this pattern of an order-$n$ HRW, has $n(n+1)-1$ non-uniform peaks. The central profile of the three breathers in Fig. 1 is very similar with the fundamental pattern of an order-3 RW [see Fig. 3(a) in Ref. [43]] of the NLS equation. The three breathers are plotted according to Theorem 1 and Corollary 1 of [48] with $a = 0.01$,$c = 0.5$, $s_0 = 0$,and $\lambda_1 = -0.2 + 0.54\mathbf{i}$ in $f_1$, $\lambda_3 = 0.1 + 0.55\mathbf{i}$ in $f_3$ and $\lambda_5 = 0.03 + 0.56\mathbf{i}$ in $f_5$.

The interaction of $n$ anti-synchronous breathers is simpler, although there also exists the fusion or fission of peaks. In the interaction area, the peaks are closer to each other. By suitable adjustment of the relative phases of the breathers, $n$ synchronous breathers become $n$ anti-synchronous breathers, and the corresponding peaks in the triangle disappear, so that only peaks in one triangle survive. Specifically, by suitably changing the relative phase, we observe the disappearance of the lowest peak in the outermost row of the interaction area, followed by the disappearance of the two nearest peaks, and so on. This chain reaction continues until the coalescence of the two triangles. The collapse of this triangle is stimulated by the loss of the nearest-neighbor interactions. Thus, there are $n(n+1)/2$ peaks in the interaction area, which are allocated on the remaining triangle. If we set $\lambda_i \mapsto \lambda_0$ simultaneously, then the profile in the interaction area of the order $n$ breather yields a triangular pattern of a HRW. Therefore, there are $n(n+1)/2$ equal-height peaks in the triangular pattern of an order-$n$ HRW. A triangular structure of the three anti-synchronous breathers is plotted in Fig. 2 by using Theorem 1 of [48] with $a = 0.01$, $c = 0.5$, and $\lambda_1 = 0.05 + 0.531\mathbf{i}$ and $s_0 = 16$ in $f_1$, $\lambda_3 = 0.55\mathbf{i}$ and $s_0 = -20\mathbf{i}$ in $f_3$, and $\lambda_5 = -0.05 + 0.551\mathbf{i}$ and $s_0 = -16$ in $f_5$. By suitably choosing different values of the parameters in $n$ anti-synchronous breathers, so that the relative positions of the peaks are changed but the total number of peaks is preserved, we obtain a ring structure associated with the $n(n+1)/2$ peaks in the interaction area, which gives rise to a circular pattern of an order $n$ RW in the above limit possessing $n(n+1)/2$ peaks. Figure 3 confirms the ring structure of three anti-synchronous breathers with $a = 0.01$, $c = 0.5$, and $\lambda_1 = 0.05 + 0.54\mathbf{i}$ and $s_0 = 1 + \mathbf{i}$ in $f_1$, $\lambda_3 = 0.55\mathbf{i}$ and $s_0 = 0$ in $f_3$, and $\lambda_5 = -0.05 + 0.56\mathbf{i}$ and $s_0 = 1 + \mathbf{i}$

in $f_5$. There exist many other patterns appearing in the interaction area of $n$ anti-synchronous breathers, which give rise to several types of HRWs such as two polygons (Fig. 4 for an order-5 RW given by Theorem 1 with $\lambda_0 = ic, a = 0, c = 1/\sqrt{2}, s_0 = 0, s_1 = 0, s_2 = 10^6$, $s_3 = 10$ for a pentagon or $s_3 = (1+I)\times 5\times 10^5$ for a heptagon, and $s_4 = 0$) and a triangle in a circle (Fig. 5 for an order-5 RW given by Theorem 1 with $\lambda_0 = ic, a = 0, c = 1/\sqrt{2}, s_0 = 0, s_1 = 15, s_2 = 0, s_3 = 0, s_4 = 10^7$).

By suitably choosing the values of the parameters in $f_i$, we observe $n$ quasi-synchronous breathers from Theorem 1 and Corollary 1 in [48]. There exist many different patterns in the interaction area, which implies many interesting types of HRWs when $\lambda_i \mapsto \lambda_0$. For example, one can find the following interesting decomposition of an order-$n$ HRW: an order -$(n-2)$ RW surrounded by $2n-1$ peaks [43]. The first nontrivial example of this decomposition is given by the interaction of four quasi synchronous breathers. Unfortunately, we are not able to plot the profile in the interaction area in this case, due to the complexity of order-4 breathers. However, we find two complete decompositions of the circular pattern: an order-5 RW in Fig. 6 with $\lambda_0 = ic, a = 0, c = 1/\sqrt{2}, s_0 = s_1 = s_2 = 0, s_3 = 8\times 10^4, s_4 = 2\times 10^7$, and an order-6 RW in Fig. 7 with $\lambda_0 = ic, a = 0, c = 1/\sqrt{2}, s_0 = s_1 = s_2 = 0, s_3 = 3\times 10^4, s_4 = 0, s_5 = 10^8$.

The inverse DT provides a technique enabling us to prove the above interesting decomposition rule of an order-$n$ RW. For simplicity we set $a = 0$ in the seed solution, and then we set $\lambda_0 = ic$. Expanding $\phi(\lambda_0 + \epsilon)$ with respect to $\epsilon$, we find that the coefficient of the first-order term in $\epsilon$ is given by

$$f_0 = \begin{pmatrix} e^{\mathbf{i}c^2t}(2\mathbf{i}cx - 4c^2t + 2\mathbf{i}cs_0 + \mathbf{i}) \\ -e^{-\mathbf{i}c^2t}(2\mathbf{i}cx - 4c^2t + 2\mathbf{i}cs_0 - \mathbf{i}) \end{pmatrix},$$

which is an eigenfunction associated with $q$ and $\lambda_0$. There exist another eigenfunction

$$g_0 = \begin{pmatrix} e^{\mathbf{i}c^2t} \\ -e^{-\mathbf{i}c^2t} \end{pmatrix}$$

of $\lambda_0$. Note that $f_0$ and $g_0$ are two linearly independent eigenfunctions of $\lambda_0$. According to Theorem 1, an order-$n$ RW is generated by a degenerate $n$-fold DT with the critical eigenvalue $\lambda_0$ from the periodic seed $q = ce^{2\mathbf{i}c^2}$. Let $T_{n-1}$ be an $(n-1)$-fold degenerate DT with $\lambda_0$, so that $g_0^{[n-1]}$ and $f_0^{[n-1]}$ are given by eq.(2), and are linearly independent. By a tedious asymptotic analysis we find that $f_0^{[n-1]} = \tilde{f}_0 + s_{n-1}g_0^{[n-1]}$, where $\tilde{f}_0$ is a smooth bounded function. According to Theorem 2, the $n$-th fold DT defined by $T(\lambda; g_0^{[n-1]})$ is the inverse of the $(n-1)$-th DT defined by $T(\lambda; f_0^{[n-2]})$. Thus, by the limit $s_{n-1} \mapsto \infty$, the $n$-th fold DT $T(\lambda; f_0^{[n-1]}) = T(\lambda; g_0^{[n-1]})$, gives an inverse transform of the $(n-1)$-th fold DT. Therefore, under this limit, an order-$n$ RW $q^{[n]}$ is reduced to an order-$(n-2)$ RW, $q^{[n-2]}$. By taking $s_{n-1}$ to be large (but finite), an order $n$ RW is decomposed into an order-$(n-2)$ RW and $2n-1$ peaks located on an outer circle such that the total number $n(n+1)/2$ of peaks can be realized either in a triangular pattern or in a circular pattern. The inner order-$(n-2)$ RW can take any of these forms by choosing $s_i (i = 0, 1, \cdots, n-3)$. This decomposition rule of HRWs was conjectured by Akhmediev and co-workers [43]. Figures 5 and 6 show different patterns of the inner lower order RW decomposed from an order-5 RW. The fundamental pattern of the inner order-3 RW reduced from an order-5 RW is shown in Fig. 4(c) of [43]. According to this decomposition rule, Figs. 6 and 7 provide the first two non-trivial examples of a complete decomposition associated with three levels.

In order to show the applicability of the generating mechanism, we present new types of decomposition of the seventh order, eighth order and ninth order RWs in Figs. 8-13. In these figures, $\lambda_0 = ic, a = 0, c = 1/\sqrt{2}$, and the other non-zero parameters are $s_6 = 10^{10}c_0$ in Fig. 8; $s_6 = 10^{10}c_0, s4 = 10^5c_0, s_2 = 10c_0$ in Fig. 9; $s_7 = 10^{10}c_0$ in Fig. 10; $s_7 = 10^{10}c_0, s5 = 10^6c_0$ in Fig. 11; $s_8 = 10^{12}c_0$ in Fig. 12; $s_8 = 10^{12}c_0, s_6 = 10^5c_0$ in Fig. 13, where $c_0 = 5 + 5\mathbf{i}$. In particular, Figs. 9 and 11 provide the first two non-trivial examples of a complete decomposition associated with four levels.

**Conclusion** The central theme of this paper is an attempt to elucidate how normal waves can evolve into a rogue wave. It is well known that when a classical envelope soliton interacts with a background plane wave, then a breather is formed [4]. Thus, there exist different types of breathers, depending on the various combinations of envelope solitons and background plane waves. It has been predicted that the maximum wave field generated due to the interaction of an envelope soliton with a background plane wave, depends on the linear superposition between the amplitudes of the soliton and the background plane wave. The problem of early detection of rogue waves is a challenging task. Indeed, since the NLS breathers are homoclinic orbits, even the slightest perturbation resulting from roundoff errors during numerical simulation, can trigger a false rogue like behavior. Akhmediev *et al.* [50] have devised a model for early detection of rogue waves in a chaotic field, which would help marine travel in stormy conditions, as it would provide an early warning system for rogue waves. Just before the appearance of the high-peak wave in real space, the spectra of unit patches of the chaotic wave fields show a specific triangular feature. Thus, the analysis of the formation of such specific features could help the early detection of rogue waves.

The two conjectures described in this article elucidate the formation of higher-order rogue waves. By understanding the generating mechanism for higher order rogue waves as a result of the fission and the fusion of $n$ degenerate breathers, the formation of the desired triangular pattern (and of a new class of circular pattern reported in this paper) is a basic features of rogue waves, which may have an important impact on their early detection. The constructions of specific triangular and circular patterns provide simple implementations of the generic results presented in this paper.

**Acknowledgements** This work is supported by the NSF of China under Grants No.10971109 and No.11271210, the K.C.Wong Magna Fund in Ningbo University and the Natural Science Foundation of Ningbo under Grant No.2011A610179. We thank Professor Yishen Li(USTC,Hefei,China) for his useful suggestions on rogue

waves and also thank Shuwei Xu, Linling Li, Lijuan Guo, Yongshuai Zhang for their help with figures. KP wishes to thank the DST, DAE-BRNS, UGC and CSIR, Government of India, for the financial support. A. S.F. is grateful to EPSRC,UK, and to the Onassis foundation, USA, for their generous support.

[1] P.C.Liu, Geofizika 24(2007),57-70.
[2] L. Draper, Oceanus 10(1964), 13-15; L. Draper, Marine Observer 35(1965), 193-195.
[3] R.G. Dean, Freak waves: A possible explanation, in Water Wave Kinematics, Edited by A.Torum and O.T. Gudmestad (Kluwer Academic, Dordrecht, 1990), pp. 609-612.
[4] C.Kharif, E.Pelinovsky and A.Slunyaev: *Rogue Waves in the Ocean*(Berlin: Springer) (2009).
[5] A.R.Osborne, Nonlinear ocean waves and the inverse scattering transformation (Academic Press, San Diego,2010).
[6] D.H. Peregrine, J. Austral. Math. Soc. B 25(1983), 16-43.
[7] D. R. Solli, C. Ropers, P. Koonath,B. Jalali, Nature(London)450(2007),1054-1058.
[8] D. R. Solli, C. Ropers, B. Jalali,Phys. Rev. Lett.101(2008),233902.
[9] J. M. Dudley, G. Genty, B.J. Eggleton, Opt. Express 16(2008), 3644-3651.
[10] A. N. Ganshin, V. B. Efimov, G.V. Kolmakov, L. P. Mezhov-Deglin,P.V. E. McClintock, Phys.Rev.Lett.101(2008),065303.
[11] Yu. V. Bludov, V. V. Konotop,N. Akhmediev,Phys.Rev.A.80 (2009),033610.
[12] M.S. Ruderman,Eur. Phys. J. Special Topics 185(2010), 57-66.
[13] W.M.Moslem, P.K.Shukla, B.Eliasson, Euro. phys. Lett.96(2011),25002.
[14] R. Höhmann, U. Kuh, H.-J. Stockmann, L. Kaplan, and E. J. Heller, Phys. Rev. Lett. 104 (2010),093901.
[15] M. Shats, H. Punzmann, H. Xia, Phys. Rev. Lett. 104(2010),104503.
[16] S.Vergeles, S.K.Turitsyn,Phys.Rev.E83(2011),061801(R).
[17] F. T. Arecchi, U. Bortolozzo, A. Montina, and S. Residori, Phys.Rev.Lett. 106(2011), 153901
[18] R.Y. Chiao, E. Garmire, C.H. Townes, Phys.Rev. Lett. 13(1964), 479-482; V.E. Zakharov,J. Appl. Mech. Tech. Phys. 9(1968), 190-194; V.E. Zakharov, and A.B. Shabat, Sov. Phys. JETP 34 (1972), 62-69.
[19] N. Akhmediev, A. Ankiewicz, M. Taki,Phys. Lett. A 373(2009), 675-678.
[20] B. Kibler, J. Fatome, C. Finot, G. Millot, F. Dias, G. Genty,N. Akhmediev,J. M. Dudley, Nature Phys.6(2010),790-795.
[21] A.Chabchoub, N.P.Hoffmann, and N.Akhmediev, Phys. Rev. Lett.106(2011),204502.
[22] H. Bailung, S.K.Sharma, and Y. Nakamura, Phys. Rev. Lett. 107(2011),255005.
[23] A.Chabchoub, N.P.Hoffmann, M. Onorato, and N.Akhmediev,Phys. Rev.X 2(2011), 011015.
[24] A. Ankiewicz, J. M. Soto-Crespo, N. Akhmediev, Phys. Rev. E. 81(2010), 046602.
[25] Y.S.Tao ,J.S. He,Phys. Rev. E. 85(2012),026601.
[26] S.W.Xu, J.S. He, L.H.Wang, J. Phys. A 44 (2011), 305203.
[27] S.W.Xu, J.S.He,J. Math. Phys.53(2012), 063507.
[28] J.S. He, S.W, Xu, K. Porsezian, J. Phys. Soc. Jpn. 81 (2012),033002.
[29] A.Ankiewicz, N.Akhmediev,J. M. Soto-Crespo, Phys. Rev. E. 82(2010),026602.
[30] B.L.Guo, L.M.Lin,Chin.Phys.Lett.28(2011), 110202.
[31] F. Baronio, A. Degasperis, M. Conforti,S. Wabnitz,Phys.Rev. Lett.109(2012),044102.
[32] B.G Zhai, W.G. Zhang, X.L. Wang, H.Q. Zhang, Nonlinear Analysis: RWA14(2013),14-27.
[33] C.Kalla, J.Phys.A44(2011),335210.
[34] Y. Ohta, J.K.Yang,Phys.Rev.E 86(2012), 036604.
[35] P. Dubard, P. Gaillard, C. Klein, V.B. Matveev,Eur. Phys. J. Special Topics 185(2010), 247-258.
[36] P. Dubard, V. B. Matveev, Nat. Hazards Earth Syst. Sci. 11(2011), 667-672.
[37] P. Gaillard,J. Phys. A 44 (2011), 435204.
[38] P. Gaillard, Eighth Peregrine breather solution of the NLS equation and multi-rogue waves(halshs-00664052, 2012.1 preprint).
[39] A. Ankiewicz, D.J. Kedziora, N. Akhmediev,Phys. Lett. A 375(2011), 2782-2785.
[40] B.L.Guo, L.M.Ling, Q.P.Liu, Phys.Rev.E 85(2012), 026607.
[41] D.J. Kedziora, A. Ankiewicz, N. Akhmediev, Phys. Rev. E 85(2012), 066601.
[42] Y. Otha, J.K.Yang, Proc.R.Soc.A 468(2012),1716-1740.
[43] D.J. Kedziora, A. Ankiewicz, N. Akhmediev, Phys. Rev. E 84(2011), 056611.
[44] N. Akhmediev, V. M. Eleonskii, N.E.Kulagain, Sov.Phys. JETP 62(1985), 894-899.
[45] J.S.He,M. Ji, Y.S.Li,Chin. Phys. Lett. 24(2007), 2157-2160.
[46] G. Neugebauer, R. Meinel, Phys. Lett. A.100(1984), 467-470.
[47] V. B. Matveev and M.A. Salle, *Darboux Transfromations and Solitons* (Springer-Verlag: Berlin,1991).
[48] J.S.He, L.Zhang, Y.Cheng, Y.S.Li, Sci.China Series A.49(2006), 1867-1878.
[49] N. Akhmediev, J.M.Soto-Crespo, A. Ankiewicz, Phys.Rev.A 80(2009), 043818.
[50] N. Akhmediev , Jose M. Soto-Crespo , A. Ankiewicz, N. Devine, Phys. Lett. A 375 (2011),2999-3001.

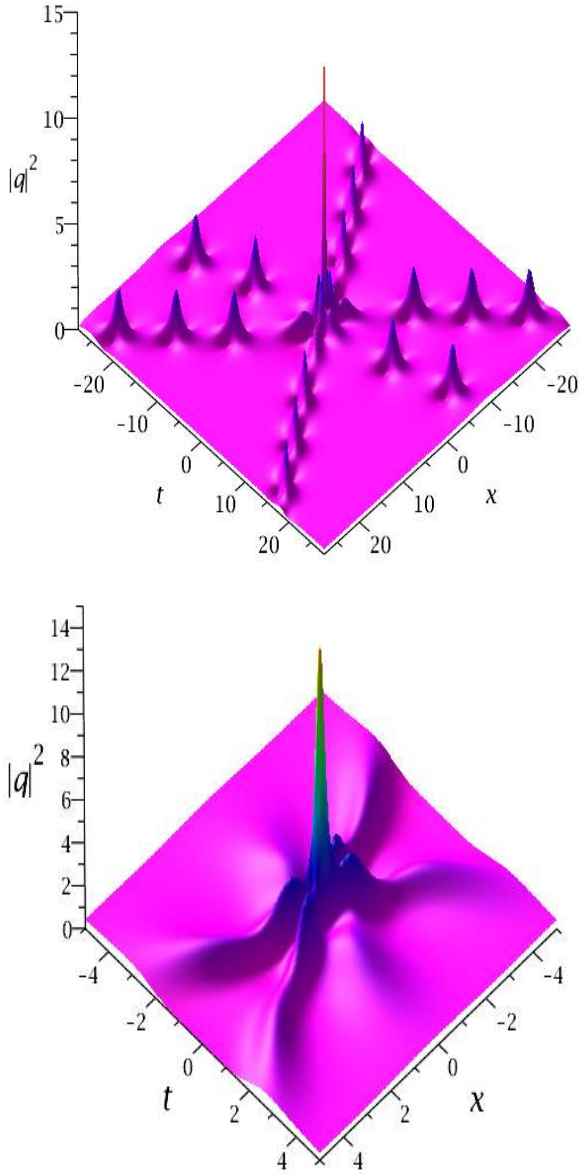


Fig. 1: (Color online) The fusion and fission of three synchronous breathers on the $(x, t)$ plane. The lower panel is a local profile in the interaction area of the upper panel

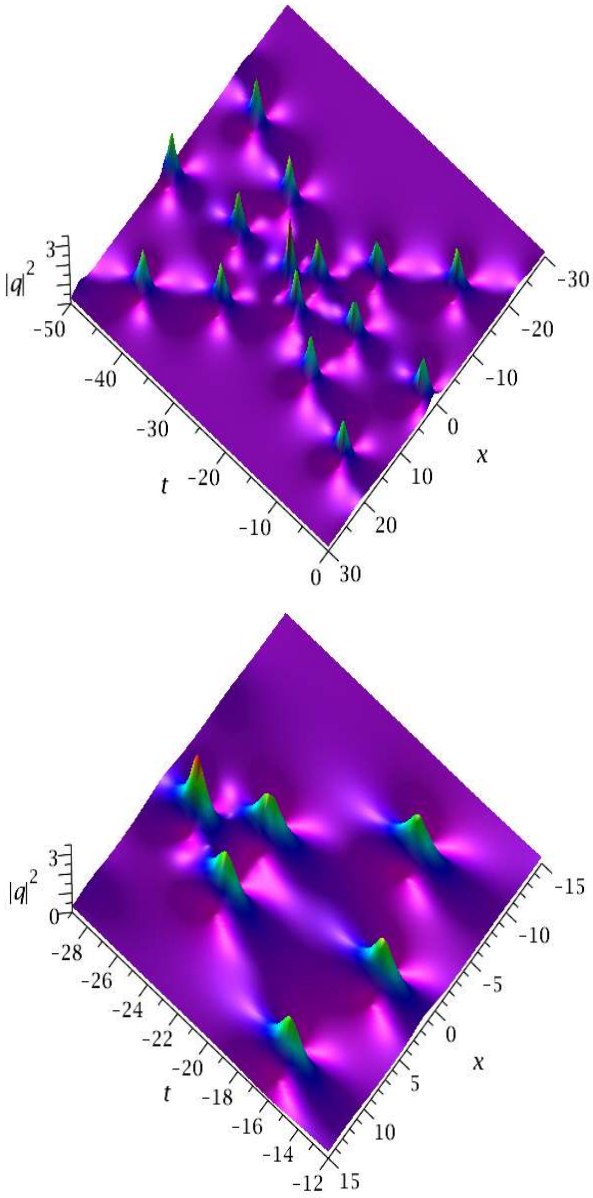


Fig. 2: (Color online) The fusion and fission of three anti-synchronous breathers on the $(x, t)$ plane. The lower panel is a local triangle pattern in the interaction area of the upper panel.

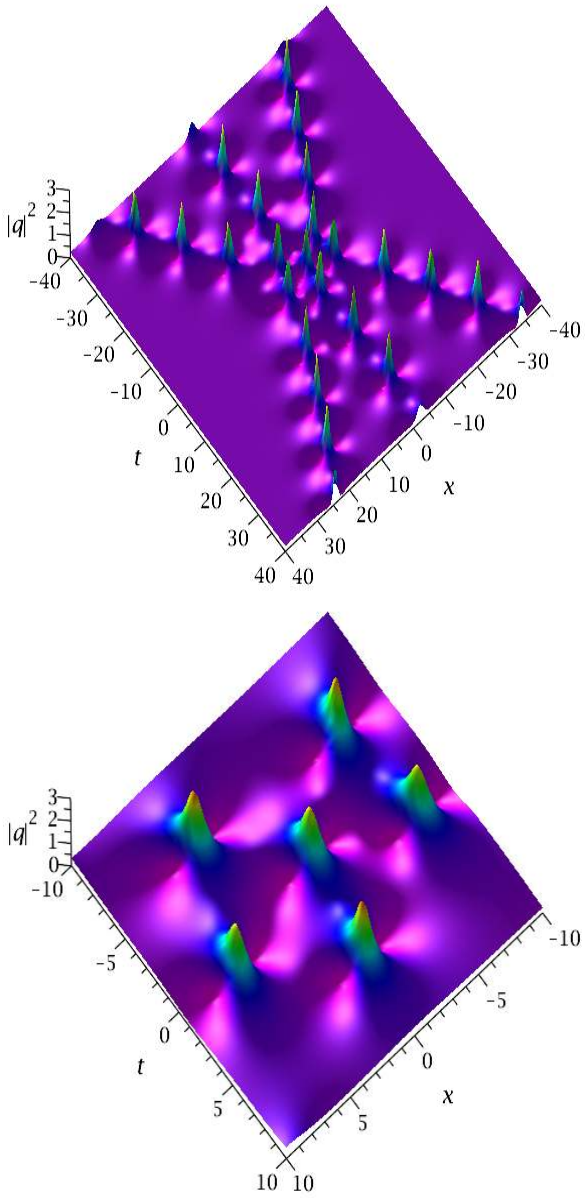


Fig. 3: (Color online) The fusion and fission of three anti-synchronous breathers on the $(x, t)$ plane. The lower panel is a local circular pattern in the interaction area of the upper panel.

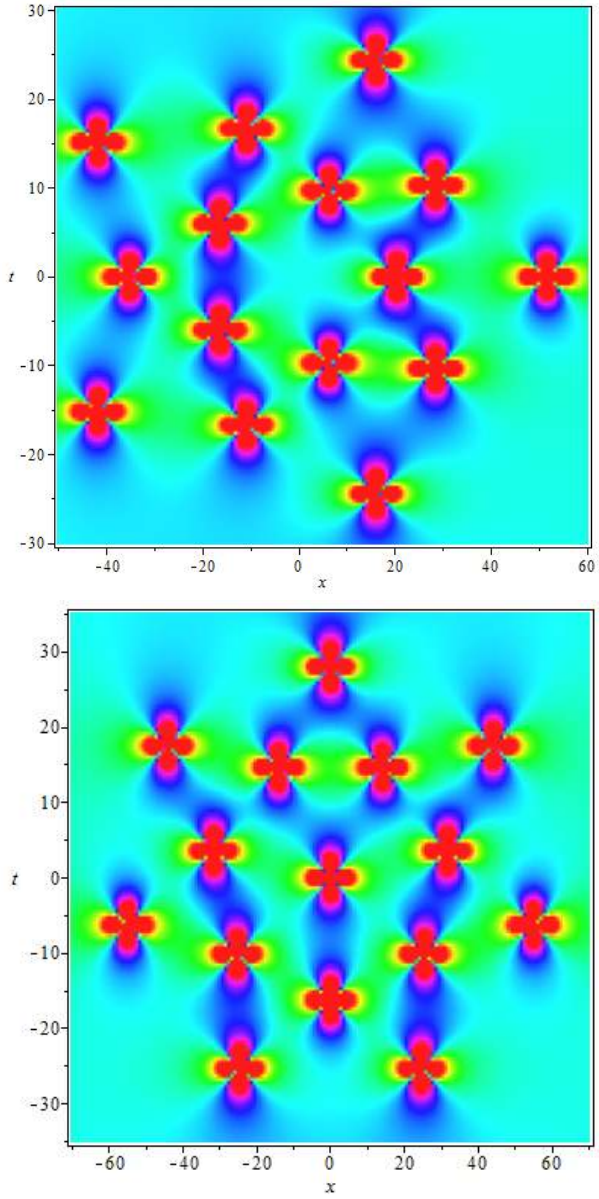


Fig. 4: (Color online) The polygon pattern of an order-5 RW. The upper pentagon has three concentric circles, and each of them has five peaks. The lower heptagon has two concentric circles, and each of them has seven peaks.

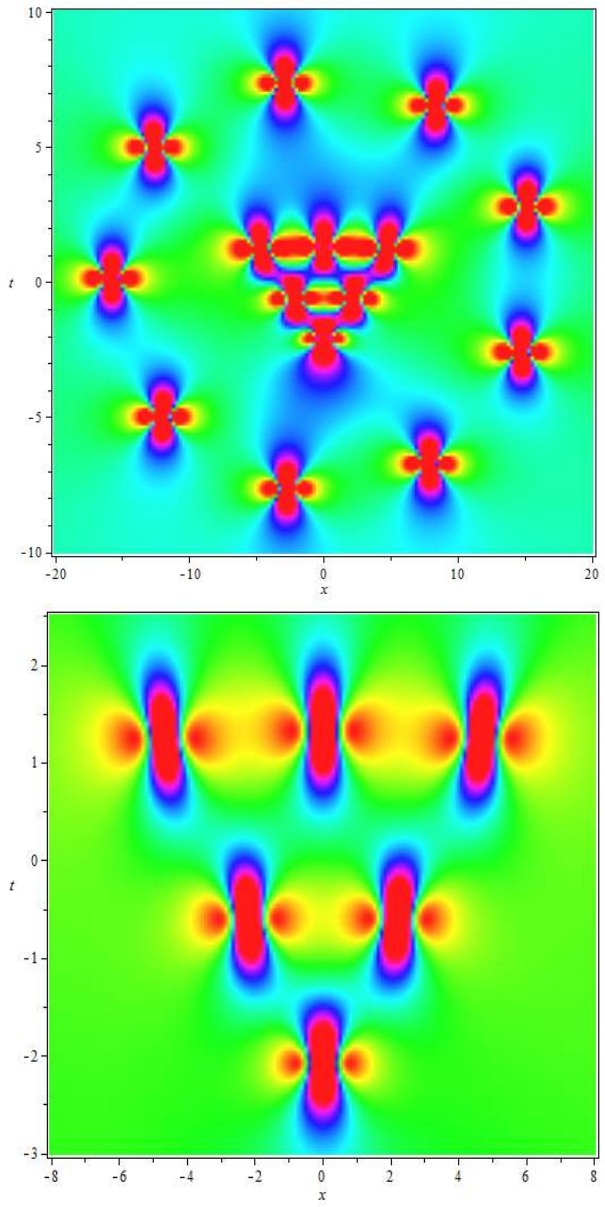


Fig. 5: (Color online) A triangle pattern in a circle for an order-5 RW. The lower panel is a local central profile of the upper panel.

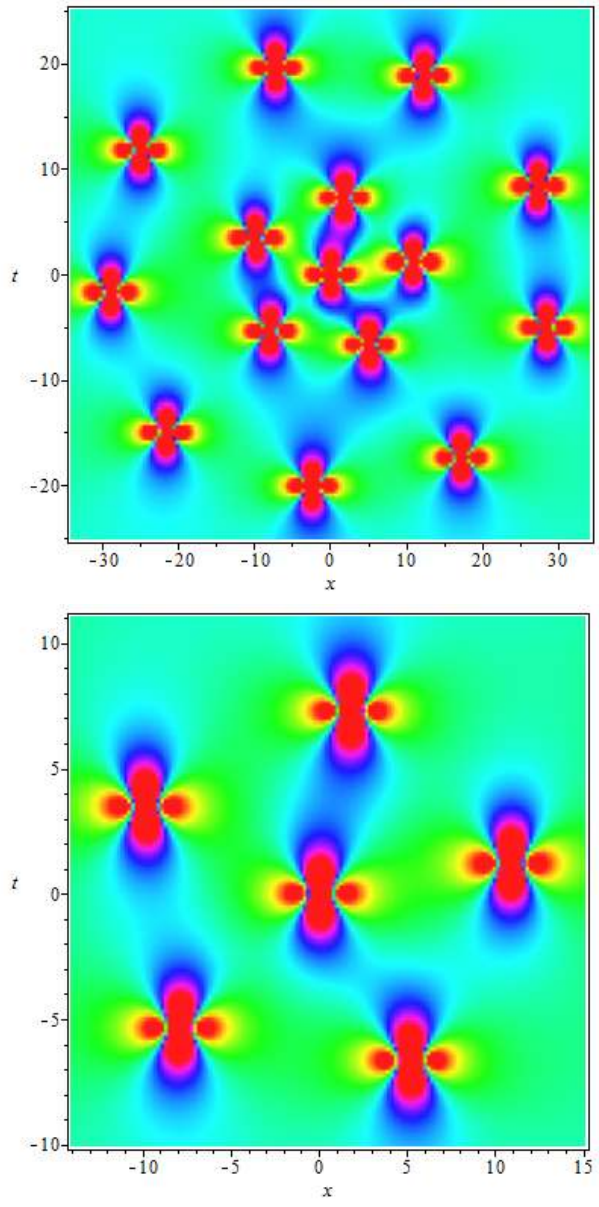


Fig. 6: (Color online) Decomposition of an order-5 RW. The lower panel is a local central profile of the upper panel.

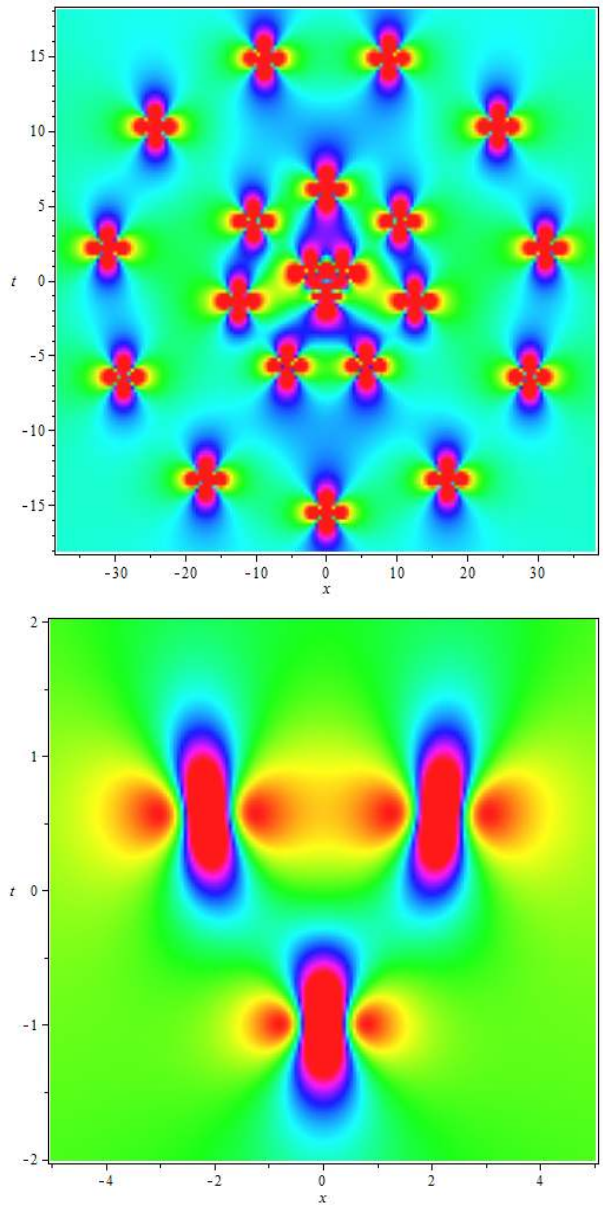


Fig. 7: (Color online) Decomposition of an order-6 RW. The lower panel is a local central profile of the upper panel.

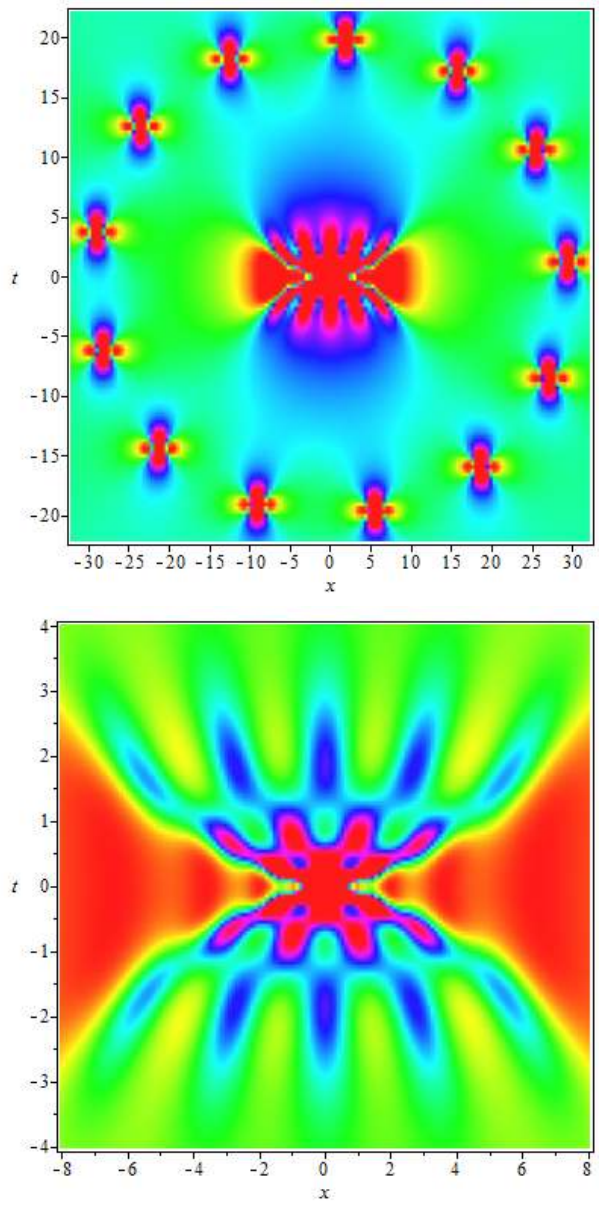


Fig. 8: (Color online) Decomposition of an order-7 RW. The lower panel is a local central profile of the upper panel.

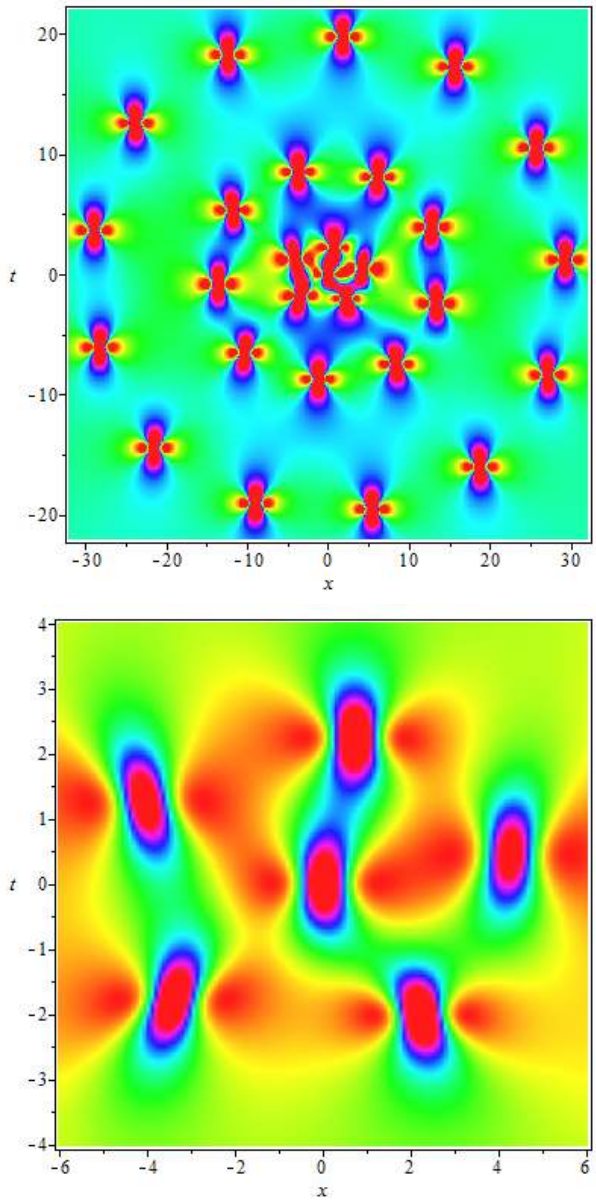


Fig. 9: (Color online) Decomposition of an order-7 RW. The lower panel is a local central profile of the upper panel.

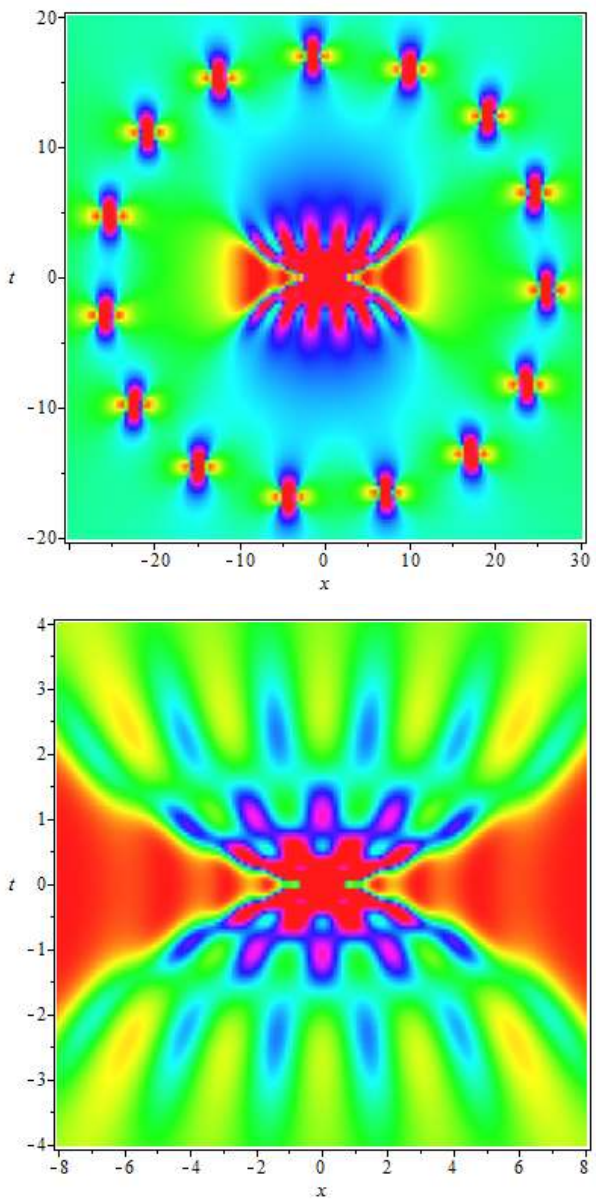


Fig. 10: (Color online) Decomposition of an order-8 RW. The lower panel is a local central profile of the upper panel.

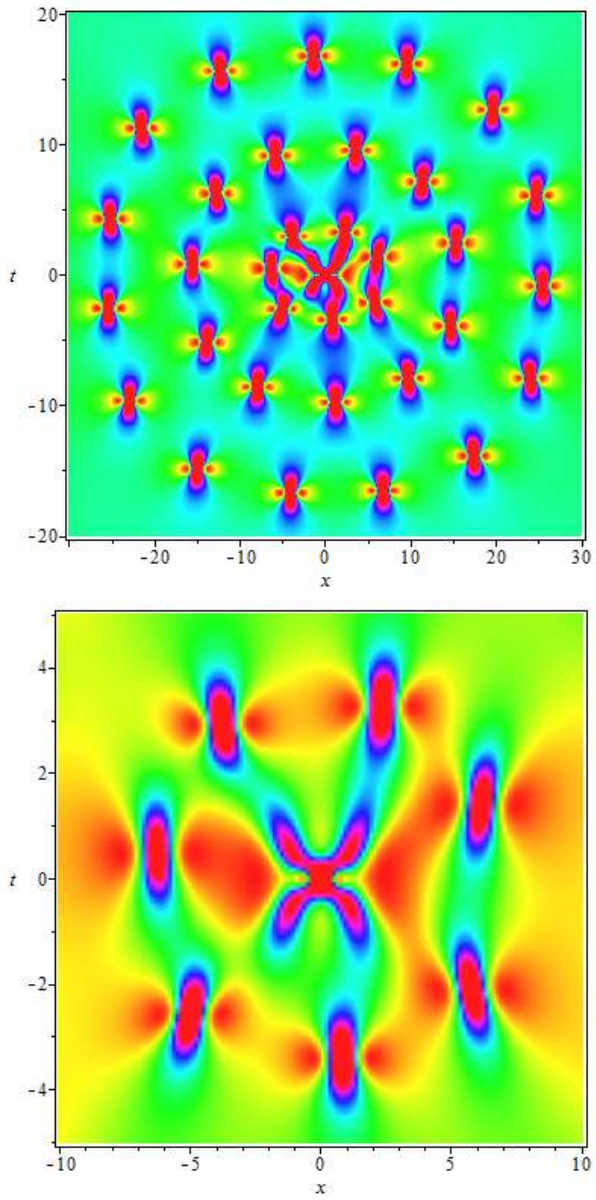


Fig. 11: (Color online) Decomposition of an order-8 RW. The lower panel is a local central profile of the upper panel.

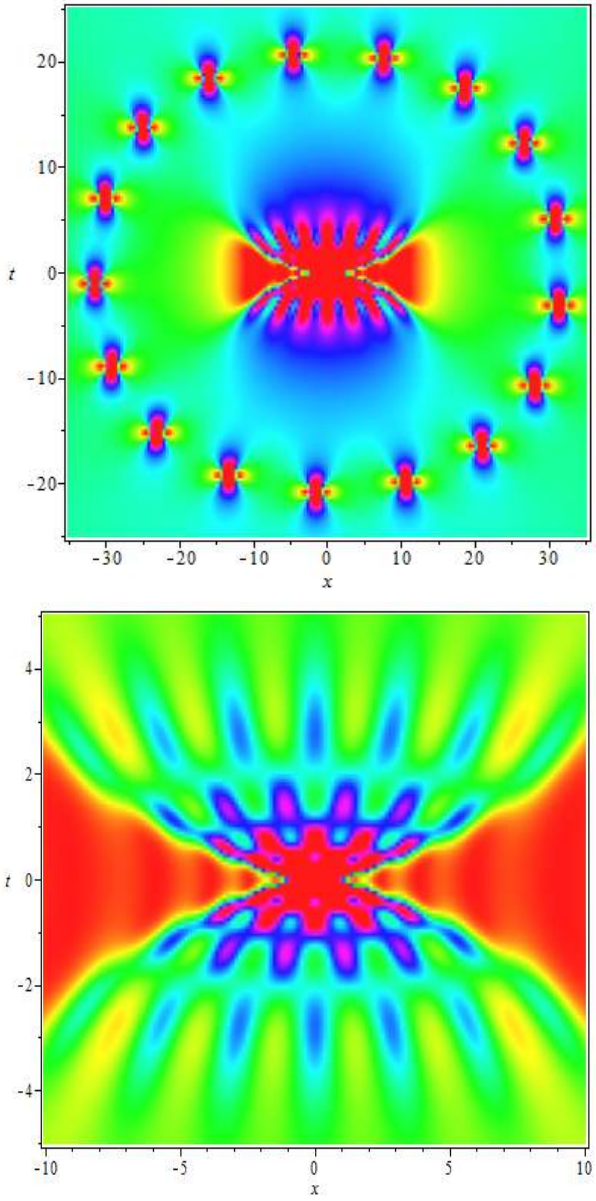


Fig. 12: (Color online) Decomposition of an order-9 RW. The lower panel is a local central profile of the upper panel.

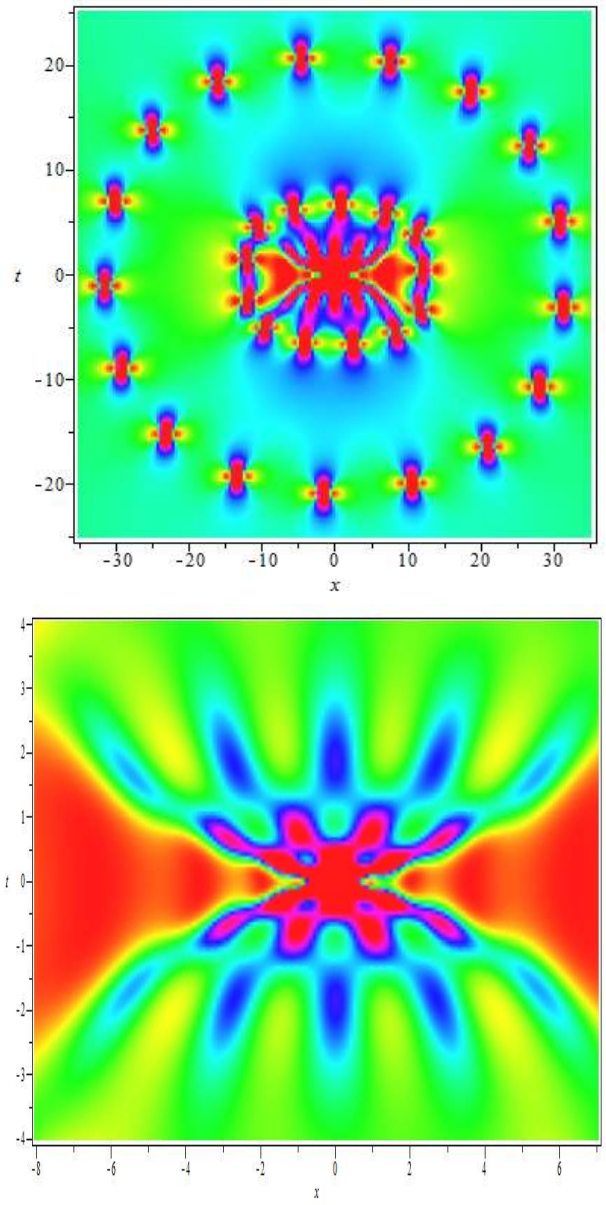


Fig. 13: (Color online) Decomposition of an order-9 RW. The lower panel is a local central profile of the upper panel.